

REVIEW OF EMITTANCE AND STABILITY MONITORING USING SYNCHROTRON RADIATION MONITORS

K.Hollmack, J.Feikes and W.B. Peatman, BESSY, Berlin, Germany

Abstract

Different techniques of emittance and stability monitoring using bend magnet and undulator radiation will be reviewed. Besides imaging methods for emittance monitoring, the problem of XBPM's used for the measurement of the centre of mass position of the undulator beams will be treated in detail. The key feature of these monitors is a careful electron optical design to take account of gap dependent changes of the shape and photon energy of the undulator beam as well as spurious signals from dipoles and high heat load. The reason for the fact that these monitors work well on low energy machines like BESSY II but often fail due in high energy machines will be demonstrated by experimental results obtained on different types of BESSY II insertion devices such as undulators, wavelength shifters, multipole wigglers and electromagnetic undulators. Experimental results of global and local orbit monitoring and a proof of principle of a XBPM-based local feedback will be shown.

1 INTRODUCTION

Experiments with Synchrotron Radiation (SR) which make use of the low emittance of the electron beam on third generation storage rings are closely related to stored beam parameters. Early predictions that orbit fluctuations of the order of 1/10 of the beam's emittance dimensions [1] can be significant have been confirmed also at BESSY II where the opening angle of the monochromatic photon beam in insertion device beam lines is dominated by the electron beam divergence rather than by the photon beam itself. For a nominal vertical opening angle of the electron beam of 25 μ rad and 20 μ m beam size at 1% coupling in the BESSY II high beta straight sections an orbit stability of 2.5 μ m and 2 μ rad is required. Hence, vertical emittance changes of 5 pmrad can already be a problem in particular for high resolution monochromators, where the source is stigmatically imaged to a slit of the order of 10 μ m or less. The horizontal stability is usually a factor of 10 more relaxed due to the larger horizontal beam shape and/or divergence and due to the fact that the monochromators usually work with vertical dispersion.

In order to measure and eventually to stabilise the beam to these small values, several types of optical monitors in addition to the usual machine diagnostics have been designed and used at other facilities. Here, after a short review, experiences with optical emittance monitors and a review of high heat load photon beam position monitors

(XBPM) and their present status together with results obtained on BESSY II will be presented.

2 OPTICAL SOURCE SIZE AND EMITTANCE MONITORS

2.1 Basic designs

The design parameters for the measurements of the beam cross section and divergence by means of SR can be estimated according to a theoretical work of Hoffmann and Meot [2]. Applying the formulas therein to third generation storage rings it becomes clear that a simple optical image of the beam in the visible is diffraction limited and yields only a blurred information for beam sizes less than about 100 μ m because of the angular aperture produced by the beam itself. In order to overcome the limit given by Fraunhofer diffraction one has to image the beam with shorter wavelengths to achieve a resolution of 10 μ m or less [3] or to use interference methods utilising the spatial coherence of SR to obtain the beam size indirectly [4]. For a fast direct X-ray imaging, however, the quality of the optics (slope errors), aberrations as well as the heat load stability of the optics has to be rather high to preserve the diffraction limited resolution which can be of the order of 1 μ m depending on the wavelength and the type of optics employed.

Several kinds of X-ray and VUV optics have been used for this purpose: Grazing incidence optics in a Kirkpatrick-Baez mirror scheme at the ALS diagnostic beamline [5], crystal based X-ray Bragg-Fresnel lenses at the ESRF [6-7]. X-ray transmission zone plates at the APS [8-9]. At BESSY, multilayer Bragg-Fresnel lenses have been tested at BESSY I and installed in the first diagnostic front end at BESSY II [10]. A monitor based on a transmission zone plate is being installed for the SLS storage ring [11]. Another type of X-ray optics, the pinhole camera, which was in operation at BESSY I from 1993 to 1999 [12] and since the first day of commissioning of BESSY II [13]. It has been successfully used at the ESRF [13] and at the APS [14] for a routine observation of the source point in a dipole and was used to determine the emittance from an undulator source [15]. At BESSY, the system was updated to a pinhole array such that a regular array of images of the dipole beam can be used to obtain the vertical divergence as well as the beam size simultaneously [10]. Presently, there are three such monitors at different source points in the BESSY II

ring featuring a diffraction limited resolution of $11\mu\text{m}$. This is close to the principle resolution limit of the pinhole camera but small enough to obtain quantitative information of the source size of usually $50\mu\text{m}$ rms on the dipole. At high energy machines the vertical photon beam divergence can be less than the angular acceptance of the pinhole and the images have to be corrected [13]. For BESSY dipoles with $1/\gamma=0.3$ mrad at 1.7 GeV this is not the case but it can be a problem trying to image a high energy undulator source with a pinhole because here the divergence is reduced by $N^{-1/2}$, where N is the number of periods.

2.2 Experiences at BESSY II

The Bragg-Fresnel Monitor as described in detail in [10] has a high nominal image resolution of $3\mu\text{m}$ and yields high quality images of the source as depicted in figure 1. Besides the image of the electron beam circular background structures arising from zero order reflection of the two lenses appear. This fact needs a sophisticated automatic image analysis to obtain correct size values. In addition, the diagnostic front end is exposed to light all the time leading to long term damage of the multilayer lenses by surface contamination due to pressure spikes (commissioning shifts) and a long term degradation of the multilayer, although it was actively cooled. After substituting the first lens, the system can be now used on request by opening a special shutter. Much better reliability despite of somewhat less resolution has been obtained using the pinhole array monitors. Vertical emittance changes of 3pmrad and position changes of $2\mu\text{m}$ can be detected using a fast image analysis of the source size. The data are logged via EPICS and together with the measured lattice parameters and the emittance as determined from the source points can be monitored every 0.3 seconds.

The general experience with these monitors is that sophisticated optical systems such as Bragg Fresnel Optics are feasible for a high resolution determination of the source size, but monitors based on the pinhole camera principle are the method of choice for a fast routine monitoring if the source size expected is not smaller than $\sim 10\mu\text{m}$. An example of source images using the pinhole monitor which operates at 16keV is shown in figure 2. Also shown are monochromatic maps of the radiation cone of the U49/1 monochromator at different coupling situations (2-5%) obtained using a scannable pinhole located 13 m from the middle of the undulator in the front end together with the beamline/monochromator as detector. It indicates that the global compensation of coupling leads to a small dipole source and to high brilliance of the insertion device beam in the next upstream straight section. Usually the emittance coupling is below 2% and an increase to 5% already means a loss of 30% intensity on the U49 SGM monochromator [16].

Therefore, a steady monitoring of the source point is very crucial for a stable beamline operation here but more relaxed on other systems without entrance slits and strong demagnification of the source.

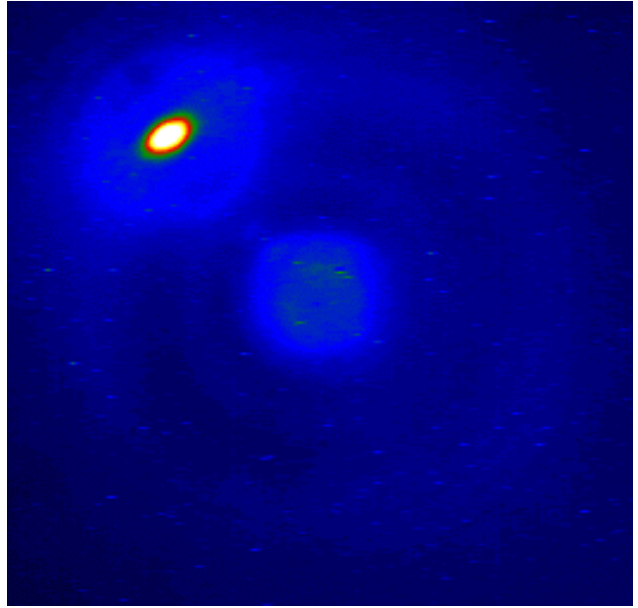


Figure 1: Source image taken with the Bragg-Fresnel-telescope before coupling was routinely compensated by skewed quadrupoles. (field of view 1.5×1.5 mm).

For a direct emittance determination from the photon beam using undulator radiation one needs to determine the source image and electron beam divergence independently as performed in [15]. At BESSY good results were achieved using monochromatic mapping of undulator angular distributions using the scannable pinhole on the blue edge of the first harmonic. The total gaussian shapes of the monochromatic beam in this blue edge case (figure 2) can be written as follows [17]:

$$\sigma^2 = \varepsilon \left(\beta + \frac{a^2}{\beta} \right) + \frac{1}{2} \left(\sigma_r^2 + a^2 \sigma_r'^2 \right) \quad (1)$$

where a is the distance to source and σ_r and σ_r' are the diffraction blurring values of size and divergence, respectively. We have to rely on the β -functions, but they are well known within a beta-beat of 10%. Moreover, it is easy to see that the most relevant term $(\beta + a^2/\beta)$ is very insensitive against absolute variations of β . The dispersion terms and additional blurring by the energy width of the beam (on higher harmonics) do not contribute here. The second term goes to zero for $\lambda \rightarrow 0$. Hence, we measured the size of the spot for different wavelengths, λ , and the beam emittance can be determined from (1) in the limit $\lambda \rightarrow 0$. The measurement was performed on the blue edges of the first harmonic while the undulator K-value (and thus, the wavelength) was varied. Here the spot has a clear 2D-gaussian shape and a 2D-gaussian fit routine was employed to obtain the

σ -values. The influence of diffraction is very small for all photon energies but using the λ -variation one obtains:

$$\varepsilon_x = (5.3 \pm 0.5) \text{ nmrad} \text{ and } \varepsilon_y = (90 \pm 30) \text{ pmrad}.$$

These values correspond to those determined from the electron beam images itself and to the design emittance of 6 nmrad of BESSY II. To check the sensitivity of the maps, coupling was introduced and the vertical blow up of the source images on the dipoles leads to a corresponding change of the maps as in figure 2. The maximum brightness of the undulator beam is achieved for the normal user run.

3 PHOTOEMISSION MONITORS (XBPM)

Synchrotron radiation monitors have been used for years to measure the intrinsic stability of the electron

beam in addition to the rf-BPMs in the ring. [18,19]. They have even been used in fast feedback loops to stabilise the electron beam [20,21]. For third generation storage rings heat load stability and reliability are key parameters if these monitors are to achieve a feedback capability. The basic technical principle was solved using thin blades of tungsten [22] or diamond [23] mounted to actively cooled copper blocks by heat conducting insulating shims. At BESSY our staggered pair monitor (SPM) concept [12,24] is successfully used for vertical position detection of dipole, wiggler and wavelength shifter radiation. They are now being implemented into the global orbit feedback which is based on rf-BPMs.

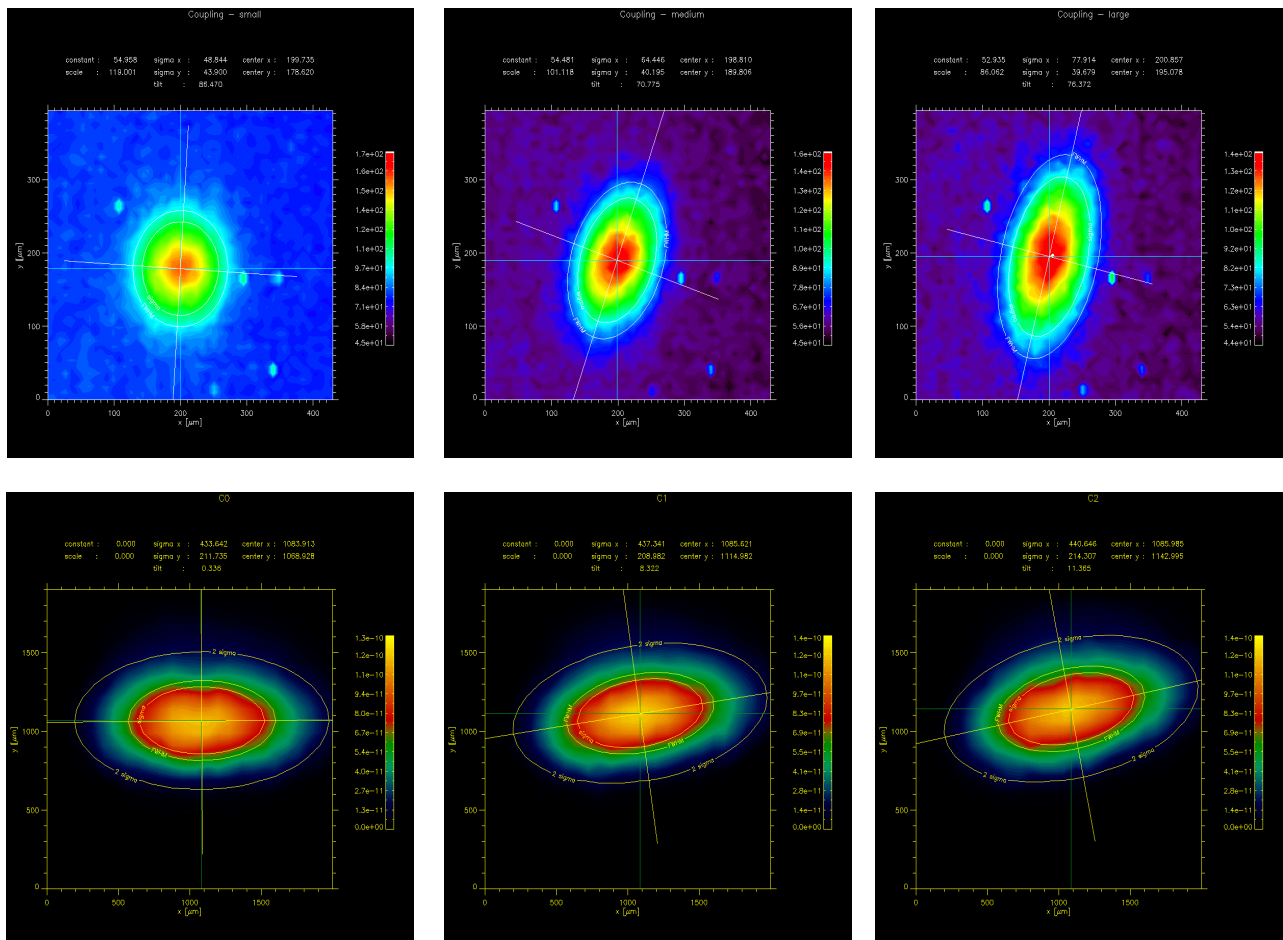


Figure 2: Comparison of the dipole source (X-ray pinhole camera) with a monochromatic map of the undulator radiation of U49/1 at the blue edge of the first harmonic at 400 eV with a bandwidth less than 10^{-4} . Emittance coupling was varied using a skewed quadrupole and is increasing from left to right. (units on the plots are in mm)

3.1 Soft X-ray undulator XBPMs

It is well known that for undulators with a variable gap the situation is quite complicated [25]. In order to optimise the resolution of the monitors, the angular and energy distribution of the undulator radiation $f(\xi, \psi, E)$ has to be weighted by the spectral efficiency of the blade material according to:

$$I(\xi, \psi) = \int f(\xi, \psi, E) q(E) dE \quad (2)$$

where $q(E)$ is the total yield of photoemission [26]. The intensity distribution the blades “see” $I(\xi, \psi)$ has then to be convoluted in space with the blade geometry (step functions) to calculate the monitor calibration curves.

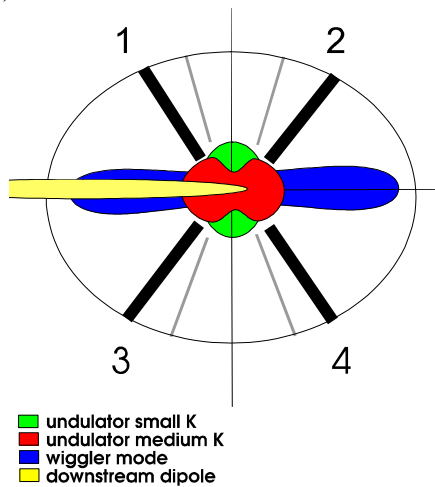


Figure 3: Polychromatic radiation pattern looking upstream into an undulator front-end. Because the dipole source is closer to the observer it is narrower than the undulator beam. (downstream blades: bold, upstream blades: light grey, vertical aperture 13 mm)

For the VUV range at BESSY this was done using the WAVE code [27]. Because $q(E)$ has significant features in the photon energy range from 1 eV to 1keV the pattern can be significantly different from the gaussian power distribution as confirmed by polychromatic mapping of BESSY II undulators [16]. For high energy undulators with first harmonics above 1keV the photoemission cross sections decrease rapidly, and that the broad band dipole radiation covering also the low energy thresholds of the blade material dominates. This is more relaxed for the VUV range but the gap dependent shape variation (medium K) as depicted in figure 3 can lead to a smaller linear range and to xy-crosstalk if the beam is not on the axis. For large K the horizontal width of $I(\xi, \psi)$ roughly increases with K/γ and the horizontal sensitivity to position changes decreases. At very small K-values the field of the undulator becomes weak and the signal of

mainly the downstream dipole radiation is left though it is geometrically separated. Measuring the usual difference over sum asymmetry A , the sensitivity versus K is as shown in figure 4 for the case of the U180 electromagnetic insertion device [28] at 1.7 GeV.

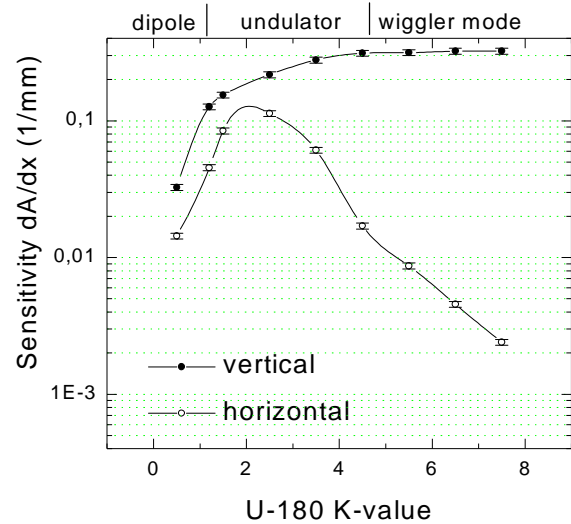


Figure 4: Sensitivity curves of a monitor XBPM 1 at 9.3 m distance from the source at U180 (PTB) of 180 mm period length (first harmonic from 5 to 100 eV).

Here, the device covers well the low energy maximum of the photoyield cross section and with increasing K the vertical sensitivity increases because it is better tuned to the central cone radiation. Below $K=1$ the low energy tail of the dipole radiation, which is far off the ring plane and off the central axis, causes a decrease both in vertical and in horizontal sensitivity. The dipole contamination ranges from 10% at low K to a few 0.1% at large K. Both, the low K and the high K tails can be influenced by discriminating low energy photoelectrons using a partial yield electron detection technique, but not the general fact that a horizontal sensitivity is available only over a limited K range. A very narrow band detection of direct photoelectrons lead to very sharp off axis features of $I(\xi, \psi)$ and thus to strong xy-crosstalk of the position response.

At BESSY the 14 operating undulator XBPMs with spectrometer option allow either the detection of indirectly detected electrons after passing a bandpass filter or a direct photoemission from the blades, where a low energy threshold can be set by a positive voltage applied to the blades. The latter needs an additional electrode in the monitor on negative voltage to avoid crosstalk. The operational experience is that the second mode is much more reliable. On some insertion devices the low energy threshold is not necessary because a geometrical suppression of the dipole background is sufficient.

3.2 Operation example

With optimised performance the monitors feature a sub-micron position resolution with the constraints above. Because their bandwidth is 2kHz they have at least vertically a feedback capability also for very tiny beam position changes arising from seismic or internally

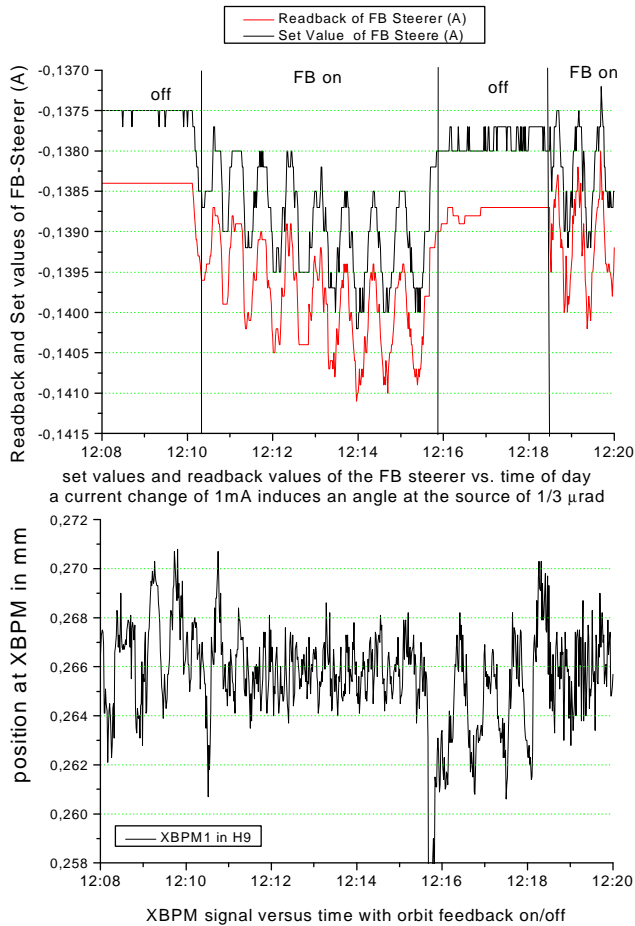


Figure 5: Local orbit feedback test at U49/1 using a closed loop realised with EPICS. The orbit was vertically corrected to the downstream XBPM 2 while the figure shows the upstream XBPM 1 signal control channel.

caused beam noise such as the 10 Hz or 50 Hz components in the beam. A proof of principle for this purpose is demonstrated below by removing the slow beam movement caused by cooling water cycles leading to peak amplitudes of 1,4 μm at the rf-BPMs and to 5 μm at XBPMs. This is residual noise not corrected by the rf-BPM based automatic global orbit feedback.

4 CONCLUSIONS

Optical beam size monitors based on X-ray pinhole camera arrays are the working horses for fast beam size and emittance determination. The BESSY solution allows them to be installed on any dipole to obtain a global online information on the source points. Imaging systems

based on X-ray or VUV-optics yield somewhat better resolution and are helpful for machine studies on very low emittance operation.

While photoemission monitors are successfully in operation at dipoles and wigglers it needs more commissioning work at undulators to find tailored settings for each individual insertion device.

REFERENCES

- [1] R.O.Hettel, Nucl. Instr. Meth. A 266 (1988) 155-163
- [2] A.Hoffmann, F.Meot, Nucl. Instr. Meth. 203 (1982) 483-493
- [3] K.Hollmack, W.B.Peatman, A.Erko and T.Noll: Nucl. Instr. Meth. (A) 365 (1995) 40-45
- [4] M.Katoh, T.Mitsuhasi, Proc. PAC'99, New York, 2307, 1999
- [5] T.R.Renner, H.A.Padmire, R.Keller, Rev. Sci. Instrum. 67 (9), 1996, p. 1
- [6] E. Tarazona et al., Rev. Sci. Instrum. 65 (6) 1994, p. 1959.
- [7] Ya. Hartman et al. Rev. Sci Instrum. 66 (2), 1995, p 1978.
- [8] Z. Cai, et al. AIP Conf. Proc., 417, AIP, (1997) p. 101
- [9] W. Yun et al., Rev. Sci. Instrum., 70, (9), 1999, p.3537
- [10] W.B.Peatman, K.Hollmack, J.Synchr.Rad. 5 (1998) 639
- [11] V.Schlott, Swiss Light Source, private commun.
- [12] K.Hollmack, W.B.Peatman, Proc. SRI'99, Stanford, CA.:AIP Conf. Proc. Vol. 521, p. 354
- [13] P. Elleaume, C. Fortgang, C. Penel, E. Tarazona, J.Synchr. Rad. (1995). 2, 209-214.
- [14] M. Borland et al., EPAC'98, Stockholm, Vol. 2 p. 1556 (1998)
- [15] B. X. Yang, A. H. Lumpkin, PAC'99, New York City, March 1999, Vol., 3, p. 2161
- [16] J. Bahrtd et al., J. Synchrotron Rad. (1998). 5, pp. 443-444
- [17] H.Wiedemann in "Particle Accelerator Physics I"
- [18] R.O.Hettel, IEEE Trans. Vol. NS-30, 2238 (1983)
- [19] L.H.Yu,R.J.Nawrocky,J.Galayda, IEEE Trans. Nucl. Sci. NS-32, 3394 (1985)
- [20] M. Bergher IEEE Trans.Nucl.Sci. Vol.NS-26,No.3,3857(1979)
- [21] R.Mortazavi et al. Nucl.Instr.Meth A, 246 (1986) 389
- [22] E.Johnson, T.Oversluizen, Rev.Sci.Instrm 60 (1989) 1947
- [23] J.Barraza,D.Shu,T.M.Kuzay, Nucl.Instr.Meth. A347 (1994)591
- [24] K.Hollmack, W.B.Peatman, PROC. SRI 2000,Berlin Nucl.Instr.Meth. A, in press
- [25] T. Warwick et al. Rev. Sci. Instr. 66 (2) 1995
- [26] J.J.Yeh: "Atomic Calculation of Photoionization Parameters", Gordon&Breach 1993
- [27] WAVE code developed by M.Scheer (BESSY)
- [28] R. Klein, J. Bahrtd, D. Herzog and G. Ulm J. Synchrotron Rad. (1998). 5, 451-452